

# Synthesis and Crystal Structure of the High-pressure Iron Borate $\beta$ -FeB<sub>2</sub>O<sub>4</sub>

Stephanie C. Neumair<sup>a</sup>, Robert Glaumb<sup>b</sup>, and Hubert Huppertz<sup>a</sup>

<sup>a</sup> Institut für Allgemeine, Anorganische und Theoretische Chemie, Leopold-Franzens Universität Innsbruck, Innrain 52a, 6020 Innsbruck, Austria

<sup>b</sup> Institut für Anorganische Chemie, Rheinische Friedrich-Wilhelms-Universität Bonn, Gerhard-Domagk-Straße 1, 53121 Bonn, Germany

Reprint requests to H. Huppertz. E-mail: Hubert.Huppertz@uibk.ac.at

Z. Naturforsch. 2009, 64b, 883–890; received June 4, 2009

The iron borate  $\beta$ -FeB<sub>2</sub>O<sub>4</sub> was synthesized under high-pressure/high-temperature conditions of 8 GPa and 1030 °C. The structure of  $\beta$ -FeB<sub>2</sub>O<sub>4</sub> is isotopic to HP-NiB<sub>2</sub>O<sub>4</sub>, representing the second example of a borate in which every BO<sub>4</sub> tetrahedron shares a common edge with a second one.  $\beta$ -FeB<sub>2</sub>O<sub>4</sub> crystallizes in the space group *C2/c* (*Z* = 4) with the parameters *a* = 950.0(2), *b* = 562.9(2), *c* = 443.7(1) pm,  $\beta$  = 108.50(3)°, *V* = 0.22495(8) nm<sup>3</sup>, *R*1 = 0.0293, and *wR*2 = 0.0647 (all data). The structure consists of layers of BO<sub>4</sub> tetrahedra, connected *via* strings of edge-sharing FeO<sub>6</sub> octahedra. A ligand field splitting of  $\Delta_o \approx 8860$  cm<sup>-1</sup> is estimated from polarized single-crystal electronic absorption spectra of  $\beta$ -FeB<sub>2</sub>O<sub>4</sub>. The tetragonal distortion of the ligand field in the [Fe<sup>II</sup>O<sub>6</sub>] chromophore amounts to  $-(8/3)d\sigma \approx 2900$  cm<sup>-1</sup>. In the range of  $16000$  cm<sup>-1</sup>  $\leq \tilde{\nu} \leq 24000$  cm<sup>-1</sup>, rather strong spin-forbidden transitions within the [Fe<sup>II</sup>O<sub>6</sub>] chromophore are observed.

**Key words:** Borate, High Pressure, Crystal Structure

## Introduction

Recent investigations in high-pressure/high-temperature syntheses of borates revealed several new compounds like the polymorphs  $\beta$ -MB<sub>4</sub>O<sub>7</sub> (*M* = Mn [1], Fe [2], Co [2], Ni [1], Cu [1], Zn [3], Ca [4], Hg [5]), the rare-earth borates RE<sub>3</sub>B<sub>5</sub>O<sub>12</sub> (*RE* = Tm–Lu [6]), and a new centrosymmetric modification of the popular nonlinear optical material bismuth triborate ( $\delta$ -BiB<sub>3</sub>O<sub>6</sub>) [7]. Two new rare-earth borates,  $\alpha$ -RE<sub>2</sub>B<sub>4</sub>O<sub>9</sub> (*RE* = Sm–Ho) [8–11] and RE<sub>4</sub>B<sub>6</sub>O<sub>15</sub> (*RE* = Dy, Ho) [8, 12, 13], exhibit edge-sharing BO<sub>4</sub> tetrahedra, a new structural motif in the chemistry of oxoborates. This motif could also be found in HP-NiB<sub>2</sub>O<sub>4</sub> [14], which is the first borate to show exclusively BO<sub>4</sub> tetrahedra sharing one common edge with a second one. Latest investigations in the system Fe–B–O led to an isotype of the exceptional HP-NiB<sub>2</sub>O<sub>4</sub>, the  $\beta$ -FeB<sub>2</sub>O<sub>4</sub> presented here.

Under ambient-pressure conditions, there are six compositions in the ternary system Fe–B–O: Fe<sup>II</sup><sub>2</sub>Fe<sup>III</sup>(BO<sub>3</sub>)O<sub>2</sub> (*Pbam*: *vonsenite* [15, 16]; *P2/m*: *hulsite* [17]), Fe<sup>II</sup>Fe<sup>III</sup><sub>2</sub>(BO<sub>4</sub>)O<sub>2</sub> (*norbergite* structure) [18, 19], Fe<sup>II</sup>Fe<sup>III</sup>(BO<sub>3</sub>)O (*Pmcn*: *warwickite* structure [20, 21], *P2<sub>1</sub>/c*: distorted *warwickite* structure

[20, 22]), FeB<sub>4</sub>O<sub>7</sub> [23, 24], FeBO<sub>3</sub> [25], and Fe<sub>2</sub>B<sub>2</sub>O<sub>5</sub> [26, 27]. The polymorphic phases Fe<sup>II</sup>Fe<sup>III</sup>(BO<sub>3</sub>)O<sub>2</sub> and Fe<sup>II</sup>Fe<sup>III</sup>(BO<sub>3</sub>)O, as well as the compounds FeBO<sub>3</sub> and Fe<sub>2</sub>B<sub>2</sub>O<sub>5</sub>, are built up from trigonal-planar BO<sub>3</sub> groups. In contrast, Fe<sup>II</sup>Fe<sup>III</sup><sub>2</sub>(BO<sub>4</sub>)O<sub>2</sub> exhibits only isolated BO<sub>4</sub> tetrahedra. The compound FeB<sub>4</sub>O<sub>7</sub> shows both of these units, BO<sub>3</sub> groups and BO<sub>4</sub> tetrahedra.

Investigations in the high-pressure/high-temperature chemistry of iron borates in our research group led to the new compound  $\alpha$ -FeB<sub>2</sub>O<sub>4</sub> [28] and the already mentioned polymorph  $\beta$ -FeB<sub>4</sub>O<sub>7</sub> [2]. Both structures consist of corner-sharing BO<sub>4</sub> tetrahedra, the former being isotopic to CaGa<sub>2</sub>O<sub>4</sub> [29], CaAl<sub>2</sub>O<sub>4</sub>-II [30, 31], and  $\beta$ -SrGa<sub>2</sub>O<sub>4</sub> [32]. We now report the synthesis of a second polymorph of FeB<sub>2</sub>O<sub>4</sub>,  $\beta$ -FeB<sub>2</sub>O<sub>4</sub>, its crystal structure, and properties. Furthermore, similarities and differences to the isotypic compound HP-NiB<sub>2</sub>O<sub>4</sub> [14] and other structures are discussed.

## Experimental Section

### Synthesis

$\beta$ -FeB<sub>2</sub>O<sub>4</sub> was synthesized under high-pressure/high-temperature conditions of 8 GPa and 1030 °C in a modi-

Table 1. Crystal data and structure refinement of  $\beta$ -FeB<sub>2</sub>O<sub>4</sub> (standard deviations in parentheses).

Empirical formula	$\beta$ -FeB <sub>2</sub> O <sub>4</sub>
Molar mass, g mol <sup>-1</sup>	141.47
Crystal system	monoclinic
Space group	<i>C2/c</i>
Powder diffractometer	Stoe Stadi P
Radiation; $\lambda$ , pm	MoK $\alpha$ ; 71.073
Powder data	
<i>a</i> , pm	950.5(3)
<i>b</i> , pm	562.8(2)
<i>c</i> , pm	444.2(2)
$\beta$ , deg	108.48(3)
<i>V</i> , nm <sup>3</sup>	0.22535(8)
Single-crystal diffractometer	Stoe IPDS-I
Radiation; $\lambda$ , pm	MoK $\alpha$ ; 71.073 (graphite monochromator)
Single-crystal data	
<i>a</i> , pm	950.0(2)
<i>b</i> , pm	562.9(2)
<i>c</i> , pm	443.7(1)
$\beta$ , deg	108.50(3)
<i>V</i> , nm <sup>3</sup>	0.22495(8)
Formula units per cell	<i>Z</i> = 4
Calculated density, g cm <sup>-3</sup>	4.18
Crystal size, mm <sup>3</sup>	0.16 × 0.11 × 0.04
Temperature, K	293(2)
Detector distance, mm	50.0
Exposure time, min	8.0
Absorption coefficient, mm <sup>-1</sup>	6.5
Absorption correction	numerical [42, 43]
<i>F</i> (000), e	272
$\theta$ range, deg	4.3–30.5
Range in <i>hkl</i>	±13, -8/+7, ±5
Reflections total / independent / <i>R</i> <sub>int</sub>	1150 / 314 / 0.0265
Reflections with <i>I</i> ≥ 2 $\sigma$ ( <i>I</i> )/ <i>R</i> <sub><math>\sigma</math></sub>	296 / 0.0179
Data / ref. parameters	314 / 34
Final <i>R</i> 1/ <i>wR</i> 2 [ <i>I</i> ≥ 2 $\sigma$ ( <i>I</i> )]	0.0276 / 0.0635
Final <i>R</i> 1/ <i>wR</i> 2 (all data)	0.0293 / 0.0647
Goodness-of-fit on <i>F</i> <sup>2</sup>	1.172
Largest diff. peak and hole, e Å <sup>-3</sup>	0.64 / -0.70

fied Walker-type multianvil apparatus. A stoichiometric mixture of “FeO” (Sigma-Aldrich Chemie GmbH, Munich, Germany, 99.9%) and B<sub>2</sub>O<sub>3</sub> (Strem Chemicals, Newburyport, USA, 99.9%) in the ratio 1:1 was ground together and filled into a boron nitride crucible (Henze BNP GmbH, HeBoSint<sup>®</sup> S10, Kempten, Germany). This crucible was positioned in the center of a 14/8-assembly and compressed by eight tungsten carbide cubes (TSM-10, Ceratizit, Reutte, Austria). The pressure was applied *via* a Walker-type multianvil device and a 1000 t press (both devices from the company Voggenreiter, Mainleus, Germany). A detailed description of the assembly and its preparation can be found in refs. [33–37]. For the synthesis, the sample was compressed to 8 GPa within 1.5 h and kept at this pressure for the heating period. The temperature was increased within 10 min to 1030 °C, kept there for 5 min, and decreased to

Table 2. Atomic coordinates and isotropic equivalent displacement parameters *U*<sub>eq</sub> (Å<sup>2</sup>) for  $\beta$ -FeB<sub>2</sub>O<sub>4</sub> (space group: *C2/c*) (standard deviations in parentheses). *U*<sub>eq</sub> is defined as one third of the trace of the orthogonalized *U*<sub>ij</sub> tensor.

Atom	W.-position	<i>x</i>	<i>y</i>	<i>z</i>	<i>U</i> <sub>eq</sub>
Fe	4 <i>e</i>	1/2	0.8423(2)	1/4	0.0096(3)
B	8 <i>f</i>	0.3126(3)	0.6079(6)	0.6230(8)	0.0092(6)
O1	8 <i>f</i>	0.6464(2)	0.8480(4)	0.9774(5)	0.0083(4)
O2	8 <i>f</i>	0.3600(2)	0.5857(4)	0.9647(5)	0.0085(4)

625 °C within 15 min. The sample was cooled down to r. t. by switching off the heating, followed by a decompression period of 4.5 h. The recovered pressure medium was broken apart and the surrounding boron nitride crucible removed from the sample. The compound  $\beta$ -FeB<sub>2</sub>O<sub>4</sub> was obtained as an oxidation-sensitive, orange-brown, crystalline solid. The sample also contained the normal-pressure phase *vonsenite* (Fe<sup>II</sup><sub>2</sub>Fe<sup>III</sup>(BO<sub>3</sub>)O<sub>2</sub>) and the already known high-pressure borate  $\alpha$ -FeB<sub>2</sub>O<sub>4</sub>.

The powder diffraction pattern clearly identified  $\beta$ -FeB<sub>2</sub>O<sub>4</sub> as the main product of the high-pressure/high-temperature reaction. The elemental analysis of  $\beta$ -FeB<sub>2</sub>O<sub>4</sub> by energy dispersive X-ray spectroscopy (Jeol JFM-6500F, Jeol. Ltd, Tokyo, Japan) led to values of 12(1) % Fe (14 %), 25(3) % B (29 %), and 63(3) % O (57 %) (theoretical values in parentheses).

#### Electronic absorption spectra

The single-crystal polarized electronic absorption spectra of  $\beta$ -FeB<sub>2</sub>O<sub>4</sub> were recorded at 293 K in the NIR/Vis/UV region (5800–28000 cm<sup>-1</sup>, step width  $\Delta\lambda$ (UV/Vis) = 1 nm,  $\Delta\lambda$ (NIR) = 2 nm) using a strongly modified CARY 17 microcrystal spectrophotometer (Spectra Services, ANU Canberra, Australia). The details of the single-beam spectrometer have already been described in the literature [38, 39]. A dichroic crystal (yellow/orange) with dimensions 0.1 × 0.1 × 0.05 mm<sup>3</sup> was selected for examination. The rather noisy spectra (see Fig. 6) result from the small size and modest optical quality of the crystals available. The reference intensity was measured using a pinhole instead of the crystal mounted on an aperture.

#### Crystal structure analysis

The powder-diffraction pattern was obtained in transmission geometry, using a Stoe Stadi P powder diffractometer with monochromatized MoK $\alpha$  ( $\lambda$  = 71.073 pm) radiation. The diffraction pattern was indexed with the program ITO [40] on the basis of a monoclinic unit cell. The lattice parameters (Table 1) were calculated from least-squares fits of the powder data. The correct indexing of the pattern of  $\beta$ -FeB<sub>2</sub>O<sub>4</sub> was confirmed by intensity calculations, taking the atomic positions from the structure refinement [41].

Atom	$U_{11}$	$U_{22}$	$U_{33}$	$U_{23}$	$U_{13}$	$U_{12}$
Fe	0.0094(3)	0.0106(4)	0.0094(4)	0	0.0040(2)	0
B	0.008(2)	0.011(2)	0.008(2)	0.000(2)	0.003(2)	-0.000(2)
O1	0.0082(9)	0.0090(9)	0.008(2)	-0.0007(6)	0.0033(7)	-0.0007(7)
O2	0.0091(9)	0.0093(9)	0.007(2)	-0.0006(7)	0.0022(7)	-0.0009(7)

Table 4. Interatomic distances (pm) for  $\beta$ -FeB<sub>2</sub>O<sub>4</sub> (space group:  $C2/c$ ), based on single-crystal data (standard deviations in parentheses).

Fe–O2 (2 $\times$ )	209.5(2)	B–O2a	144.3(4)	O1–Ba	151.2(4)
Fe–O1b (2 $\times$ )	211.3(2)	B–O2b	144.3(4)	O1–Bb	152.5(4)
Fe–O1a (2 $\times$ )	225.8(2)	B–O1a	151.2(4)		av. = 151.9
	av. = 215.3	B–O1b	152.5(4)		
			av. = 148.1		

Table 5. Interatomic angles (deg) for  $\beta$ -FeB<sub>2</sub>O<sub>4</sub> (space group:  $C2/c$ ), based on single-crystal data (standard deviations in parentheses).

O2a–Fe–O2b	92.8(2)	B–O1–B	86.6(2)
O2a–Fe–O1a	94.10(8)	B–O2–B	122.3(2)
O2b–Fe–O1a	87.09(8)		av. = 104.5
O2a–Fe–O1b	87.09(8)		
O2b–Fe–O1b	94.10(8)	O2a–B–O2b	113.8(2)
O2b–Fe–O1c	94.56(8)	O2a–B–O1b	112.4(3)
O1a–Fe–O1c	79.65(8)	O2b–B–O1a	111.3(2)
O1b–Fe–O1c	99.00(7)	O2a–B–O1a	111.0(2)
O2a–Fe–O1d	94.56(8)	O2b–B–O1b	113.3(3)
O1a–Fe–O1d	99.00(7)	O1a–B–O1b	93.4(2)
O1b–Fe–O1d	79.65(8)		av. = 109.2
O1c–Fe–O1d	78.96(2)		
	av. = 90.0		

To get a single-crystal structure analysis, small irregularly shaped single-crystals of the sample were isolated by mechanical fragmentation and examined through a Buerger precession camera, equipped with an image plate system (Fujifilm BAS-1800), in order to establish both, symmetry and suitability for the intensity data collection. Measurements of the single-crystal intensity data were performed at r.t. by a Stoe IPDS-I diffractometer with graphite-monochromatized MoK $\alpha$  ( $\lambda = 71.073$  pm) radiation. All relevant details of the data collection and evaluation are listed in Table 1. In accordance with the systematic extinctions  $hkl$  with  $h + k \neq 2n$  and  $h0l$  with  $h, l \neq 2n$ , the space groups  $C2/c$  (no. 15) and  $Cc$  (no. 9) were derived. For the intensity data of  $\beta$ -FeB<sub>2</sub>O<sub>4</sub>, a numerical absorption correction was applied with the program X-SHAPE [42, 43]. Due to the isotopy of  $\beta$ -FeB<sub>2</sub>O<sub>4</sub> to HP-NiB<sub>2</sub>O<sub>4</sub>, the structural refinement could be successfully performed in the centrosymmetric space group  $C2/c$ , employing the positional parameters of HP-NiB<sub>2</sub>O<sub>4</sub> as starting values [SHELXL-97 [44] (full-matrix least-squares on  $F^2$ )]. All atoms were refined with anisotropic displacement parameters. The final difference Fourier syntheses did not reveal any significant peaks. Tables 2–5 list the positional parameters, anisotropic displacement parameters, interatomic distances, and angles.

Table 3. Anisotropic displacement parameters  $U_{ij}$  ( $\text{\AA}^2$ ) for  $\beta$ -FeB<sub>2</sub>O<sub>4</sub> (space group:  $C2/c$ ) (standard deviations in parentheses).

Further details of the crystal structure investigation may be obtained from Fachinformationszentrum Karlsruhe, 76344 Eggenstein-Leopoldshafen, Germany (fax: +49-7247-808-666; e-mail: crysdata@fiz-karlsruhe.de, [http://www.fiz-informationsdienste.de/en/DB/icsd/depot\\_anforderung.html](http://www.fiz-informationsdienste.de/en/DB/icsd/depot_anforderung.html)) on quoting the deposition number CSD-420403.

## Results and Discussion

Fig. 1 gives a view of the crystal structure of  $\beta$ -FeB<sub>2</sub>O<sub>4</sub> along  $[00\bar{1}]$ . This centrosymmetric oxoborate

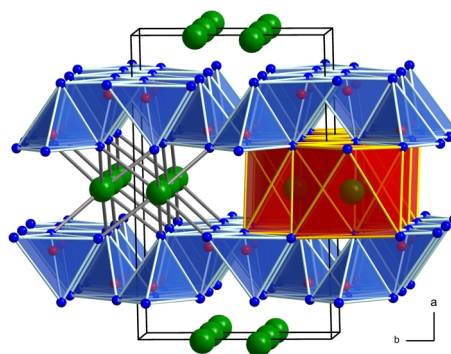


Fig. 1. (Color online). Crystal structure of  $\beta$ -FeB<sub>2</sub>O<sub>4</sub>, viewed along  $[00\bar{1}]$ . Blue polyhedra (top and bottom layer): BO<sub>4</sub> tetrahedra; red polyhedra (center layer): FeO<sub>6</sub> octahedra; green spheres (large): Fe<sup>2+</sup>; blue spheres (corners of tetrahedra): O<sup>2-</sup>; red spheres (center of tetrahedra): B<sup>3+</sup>.

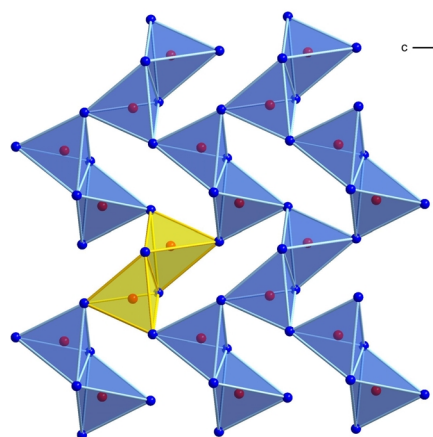


Fig. 2. (Color online). Layer of edge- and corner-sharing BO<sub>4</sub> tetrahedra in  $\beta$ -FeB<sub>2</sub>O<sub>4</sub>, viewed along  $[\bar{1}00]$ . One B<sub>2</sub>O<sub>6</sub> unit is highlighted.

is composed of distorted BO<sub>4</sub> tetrahedra. Fig. 2 shows that each of these tetrahedra is connected to a second one *via* edge-sharing, forming B<sub>2</sub>O<sub>6</sub> building blocks. These groups are interconnected *via* common vertices, resulting in layers in the crystallographic *bc* plane, that are linked by strings of edge-sharing FeO<sub>6</sub> octahedra, running along the *c* direction. Inside the layers, “sechser” rings [45] are formed by four B<sub>2</sub>O<sub>6</sub> units, each unit being part of four “sechser” rings.

As already mentioned, the structure of  $\beta$ -FeB<sub>2</sub>O<sub>4</sub> is isotypic to HP-NiB<sub>2</sub>O<sub>4</sub> [14]. Unfortunately, the designation (prefix) is not identical because this nickel borate was identified as the first compound in this structure type. When the nickel borate was synthesized under high-pressure conditions, we designated this compound with the prefix HP (*High Pressure*), because up to now, there exists no normal-pressure phase of the composition NiB<sub>2</sub>O<sub>4</sub>. In contrast, when  $\beta$ -FeB<sub>2</sub>O<sub>4</sub> was synthesized, there already existed the iron borate  $\alpha$ -FeB<sub>2</sub>O<sub>4</sub> [28], synthesized under high-pressure conditions, too. So, the here presented compound got the prefix  $\beta$  to distinguish these two polymorphs.

Besides HP-NiB<sub>2</sub>O<sub>4</sub> and  $\beta$ -FeB<sub>2</sub>O<sub>4</sub>, there are two other borate structure types with the motif of B<sub>2</sub>O<sub>6</sub> units: the rare-earth borates  $\alpha$ -RE<sub>2</sub>B<sub>4</sub>O<sub>9</sub> (RE = Sm–Ho) [8–11] and RE<sub>4</sub>B<sub>6</sub>O<sub>15</sub> (RE = Dy, Ho) [8, 12, 13].

Fig. 3 shows the interatomic angles and distances inside the B<sub>2</sub>O<sub>6</sub> unit of  $\beta$ -FeB<sub>2</sub>O<sub>4</sub>. As we could expect, the B–O distances inside the B<sub>2</sub>O<sub>2</sub> ring (B1–O1: 151.2(4), 152.5(4) pm) are longer than those outside of the “zweier” rings [45] [B1–O2: 144.3(4) pm (2 $\times$ )]. The average B–O bond length of 148.1 pm is slightly increased in comparison to the average distance in isolated BO<sub>4</sub> tetrahedra of 147.6 pm [46, 47]. Inside the B<sub>2</sub>O<sub>6</sub> unit, the B $\cdots$ B distance comes to 208.3(5) pm, which corresponds to values found in other high-

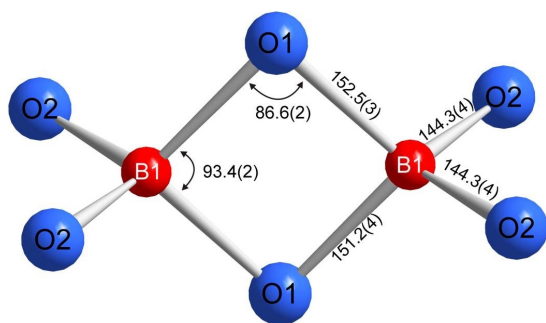


Fig. 3. (Color online). Distances (pm) and angles (deg) in the B<sub>2</sub>O<sub>6</sub> unit of  $\beta$ -FeB<sub>2</sub>O<sub>4</sub>.

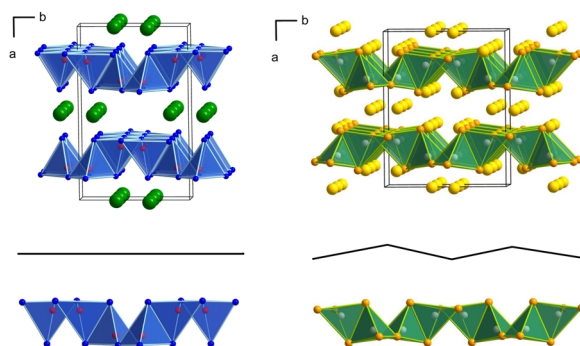


Fig. 4. (Color online). Comparison of the layer structures of  $\beta$ -FeB<sub>2</sub>O<sub>4</sub> (left) and  $\beta$ -Ca<sub>3</sub>[Al<sub>2</sub>N<sub>4</sub>] (right), viewed along [00 $\bar{1}$ ].

pressure borates exhibiting edge-sharing BO<sub>4</sub> tetrahedra, *e. g.* HP-NiB<sub>2</sub>O<sub>4</sub> (208.8(2) pm),  $\alpha$ -RE<sub>2</sub>B<sub>4</sub>O<sub>9</sub> (RE = Sm: 207.1(9); Eu: 205.3(9); Gd: 204(2); Tb: 205.5(9); Ho: 204(3) pm) [8–11], and RE<sub>4</sub>B<sub>6</sub>O<sub>15</sub> (RE = Dy: 207.2(8), Ho: 207(1) pm) [8, 12, 13].

The Fe–O distances inside the distorted FeO<sub>6</sub> octahedra vary between 209.5(2) and 225.8(2) pm and average out to 215.3 pm. As expected, these distances are slightly increased compared to the average iron oxygen distances in six-fold coordinated Fe<sup>3+</sup> ions in borates, *e. g.* in Fe<sup>II</sup>Fe<sup>III</sup><sub>2</sub>(BO<sub>4</sub>)O<sub>2</sub> (203.8 pm) [18, 19] or FeBO<sub>3</sub> (202.8 pm) [25]. The average Fe<sup>2+</sup>–O bond length of 218.5 pm for the recently published high-pressure compound  $\alpha$ -FeB<sub>2</sub>O<sub>4</sub> agrees well with the average value of  $\beta$ -FeB<sub>2</sub>O<sub>4</sub> (215.3 pm). For a more detailed description of the HP-NiB<sub>2</sub>O<sub>4</sub> structure type see ref. [14].

Similar layers of edge-sharing tetrahedra with different atoms were observed in the compounds  $\beta$ -Ca<sub>3</sub>[Al<sub>2</sub>N<sub>4</sub>] [48], Ca<sub>3</sub>[Al<sub>2</sub>As<sub>4</sub>] [49],  $\alpha$ -Ca<sub>3</sub>[Ga<sub>2</sub>N<sub>4</sub>] [50], Sr<sub>3</sub>[Al<sub>2</sub>P<sub>4</sub>] [51], and Ba<sub>3</sub>[In<sub>2</sub>P<sub>4</sub>] [52]. Due to the fact that the layers in these compounds are corrugated, and the metal content between the layers is three times as high as in  $\beta$ -FeB<sub>2</sub>O<sub>4</sub>, these structures differ substantially. Fig. 4 depicts a comparison of the layers of  $\beta$ -FeB<sub>2</sub>O<sub>4</sub> (Fig. 4 left) and  $\beta$ -Ca<sub>3</sub>[Al<sub>2</sub>N<sub>4</sub>] (Fig. 4 right).

A comparison of selected structure parameters of the isotypic structures  $\beta$ -FeB<sub>2</sub>O<sub>4</sub> and HP-NiB<sub>2</sub>O<sub>4</sub> is shown in Table 6. A closer look at the lattice parameters reveals remarkable differences in *a* ( $\beta$ -FeB<sub>2</sub>O<sub>4</sub>: 950.0(2), HP-NiB<sub>2</sub>O<sub>4</sub>: 924.7(2) pm). In contrast, the lattice parameters *b* ( $\beta$ -FeB<sub>2</sub>O<sub>4</sub>: 562.9(2), HP-NiB<sub>2</sub>O<sub>4</sub>: 552.3(2) pm) and *c* ( $\beta$ -FeB<sub>2</sub>O<sub>4</sub>: 443.7(1), HP-NiB<sub>2</sub>O<sub>4</sub>: 442.9(1) pm) show only a minor or nearly

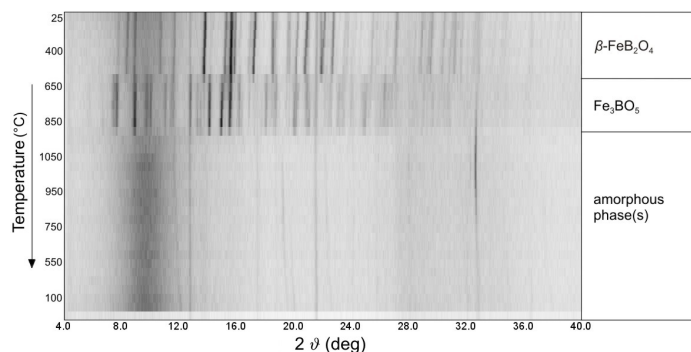


Fig. 5. Temperature-programmed diffraction patterns of  $\beta$ -FeB<sub>2</sub>O<sub>4</sub>.

Table 6. Comparison of the isotypic structures  $\beta$ -FeB<sub>2</sub>O<sub>4</sub> and HP-NiB<sub>2</sub>O<sub>4</sub> [14].

Empirical formula	$\beta$ -FeB <sub>2</sub> O <sub>4</sub>	HP-NiB <sub>2</sub> O <sub>4</sub>
Molar mass, g mol <sup>-1</sup>	141.5	144.3
Crystal system		monoclinic
Space group		<i>C2/c</i>
Unit cell dimensions:		
<i>a</i> , pm	950.0(2)	924.7(2)
<i>b</i> , pm	562.9(2)	552.3(2)
<i>c</i> , pm	443.7(1)	442.9(1)
$\beta$ , deg	108.50(3)	108.30(3)
<i>V</i> , nm <sup>3</sup>	0.225(1)	0.215(1)
B–O bond lengths, pm:		
B–O1	151.2(4), 152.5(4)	151.6(2), 153.1(2)
B–O2	144.3(4), 144.3(4)	144.5(2), 144.3(2)
av. B–O distance, pm	148.1	148.4
B···B distance in B <sub>2</sub> O <sub>6</sub> unit, pm	208.3(5)	208.8(2)
av. M–O distance, pm	215.3	208.6

no difference, respectively. The reason that the differences in the BO<sub>4</sub> tetrahedra of both compounds are negligible can be found in the ionic radii of the cations. The increased ionic radius for Fe<sup>2+</sup> leads to an enlargement of the interlayer distance in  $\beta$ -FeB<sub>2</sub>O<sub>4</sub> along *a* and a broadening of the strings of FeO<sub>6</sub> octahedra along *b*. In the *c* direction, no elongation of the strings of octahedra can be observed.

Because of the extreme synthetic conditions of 8 GPa and 1030 °C, we investigated the metastable character of the high-pressure phase  $\beta$ -FeB<sub>2</sub>O<sub>4</sub>. Temperature-programmed X-ray powder diffraction experiments were performed on a Stoe Stadi P powder diffractometer [monochromatized MoK $\alpha$  radiation ( $\lambda$  = 71.073 pm)] with a computer-controlled Stoe furnace. The sample was enclosed in a silica capillary and heated from r. t. to 500 °C in 100 °C steps, and from 500 °C to 1100 °C in steps of 50 °C. Afterwards, the sample was cooled to 500 °C in

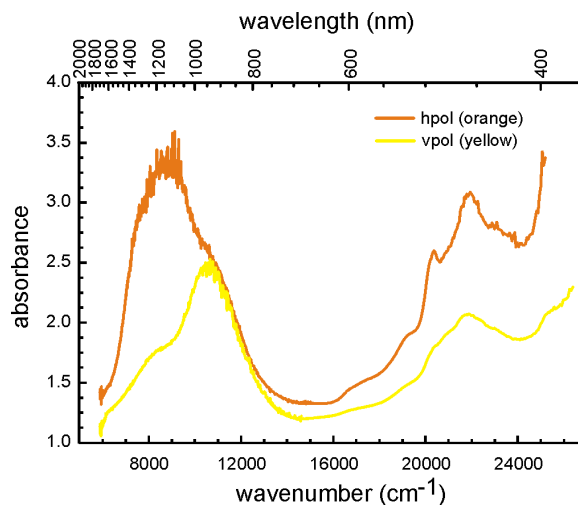


Fig. 6. (Color online). Polarized single-crystal electronic absorption spectra of  $\beta$ -FeB<sub>2</sub>O<sub>4</sub>. Crystal face not indexed; thickness  $\sim$  0.05 mm; the colors orange and yellow refer to the color of the crystal in the corresponding polarization directions.

50 °C steps, and below 500 °C in 100 °C steps. At each temperature, a diffraction pattern was recorded. Fig. 5 shows that the high-pressure phase  $\beta$ -FeB<sub>2</sub>O<sub>4</sub> remains stable up to a temperature of 500 °C. A further increase of temperature leads to the decomposition of the high-pressure phase into *vonsenite* (Fe<sup>II</sup><sub>2</sub>Fe<sup>III</sup>(BO<sub>3</sub>)O<sub>2</sub>). Above 900 °C and during cooling, no crystalline phases could be detected. The reflections visible above 900 °C are caused by the oven. The temperature-programmed X-ray powder investigations of the isotypic high-pressure phase HP-NiB<sub>2</sub>O<sub>4</sub> revealed a higher temperature stability up to 750 °C. At higher temperatures, HP-NiB<sub>2</sub>O<sub>4</sub> decomposed into the normal-pressure borate Ni<sub>3</sub>(BO<sub>3</sub>)<sub>2</sub> and presumably B<sub>2</sub>O<sub>3</sub>.

Table 7. Ligand field splittings and interatomic distances of the  $[M^{II}O_6]$  chromophores in  $\beta$ -FeB<sub>2</sub>O<sub>4</sub>, Fe<sub>2</sub>P<sub>4</sub>O<sub>12</sub>, HP-NiB<sub>2</sub>O<sub>4</sub>, and Ni<sub>2</sub>P<sub>4</sub>O<sub>12</sub>.

Compound	$\Delta_o$ (cm <sup>-1</sup> )	$-(8/3)d\sigma$ (cm <sup>-1</sup> )	$d(M-O)$ (Å)	References
$\beta$ -FeB <sub>2</sub> O <sub>4</sub>	8860	2900	2.10, 2.11, 2.26 (2×)	this work
Fe <sub>2</sub> P <sub>4</sub> O <sub>12</sub> <sup>a</sup>	~ 8700	~ 4500	2.05, 2.14, 2.20 (2×) <sup>b</sup> 2.05, 2.12, 2.20 (2×)	[54, 70]
HP-NiB <sub>2</sub> O <sub>4</sub>	8620	≤ 1500	2.05, 2.05, 2.18 (2×)	[14]
Ni <sub>2</sub> P <sub>4</sub> O <sub>12</sub>	7300	≤ 1500	1.99, 2.06, 2.07 (2×) <sup>b</sup> 1.99, 2.09, 2.12 (2×)	[55, 71]

<sup>a</sup> The powder reflectance spectrum of Fe<sub>2</sub>P<sub>4</sub>O<sub>12</sub> shows a broad band around 9200 cm<sup>-1</sup> with pronounced shoulders at 7000 and 11500 cm<sup>-1</sup> [54]; <sup>b</sup> the structure of the metaphosphates consists of two independent metal sites.

Crystals of  $\beta$ -FeB<sub>2</sub>O<sub>4</sub> show dichroism (orange/yellow). From their polarized single-crystal electronic absorption spectra, a ligand field splitting  $\Delta_o \approx 8860$  cm<sup>-1</sup> is estimated. Note that  $\Delta_o$  for tetragonally distorted chromophores containing  $d^1$ ,  $d^4$ ,  $d^6$ , or  $d^9$  ions is not identical, but slightly smaller than the average of the two absorption bands, in the case of  $\beta$ -FeB<sub>2</sub>O<sub>4</sub> observed at  $\nu = 7840$  and  $\nu = 10725$  cm<sup>-1</sup>. The energy difference between these two bands (Fig. 6) reflects the tetragonal distortion of the ligand field (and the splitting of the excited state  ${}^5E_g$ , for  $O_h$  symmetry) in the  $[Fe^{II}O_6]$  chromophore and amounts for  $\beta$ -FeB<sub>2</sub>O<sub>4</sub> to  $-(8/3)d\sigma \approx 2900$  cm<sup>-1</sup>. Assuming (in accordance with literature [53]) that the splitting of the ground state ( ${}^5T_{2g}$  for  $O_h$  symmetry) is about one quarter of the excited state, leads to our estimate of  $\Delta_o$ . This estimated value tallies well with  $\Delta_o(Fe_2P_4O_{12}) = 8700$  cm<sup>-1</sup> [54],  $\Delta_o(Ni_2P_4O_{12}) = 7300$  cm<sup>-1</sup> [55], and  $\Delta_o(HP-NiB_2O_4) = 8620$  cm<sup>-1</sup> [14]. Apparently, there is a slightly higher ligand-field splitting in the borates. We attribute this higher splitting to the higher coordination number of the ligating oxygen atoms in the borates, c. n. ( $O^{2-}$ ) = 4 in contrast to c. n. ( $O^{2-}$ ) = 2 and 3 in the metaphosphates. As a result, slightly lower  $\pi$ -bonding should be exerted by the oxygen ligands in the borates. The distortion of the  $[Ni^{II}O_6]$  and  $[Fe^{II}O_6]$  octahedra in the borates and the metaphosphates is quite similar (Table 7). Therefore, we have to note that the tetragonal splitting of the ligand field, as it is observed from the electronic absorption spectra, is much higher for the  $[Fe^{II}O_6]$  chromophores. We believe that this effect follows from a strong vibronic coupling in the iron(II) compounds, as already discussed in the literature [53]. Our attempts to model the observed  $d-d$  transition energies for  $\beta$ -FeB<sub>2</sub>O<sub>4</sub> and Fe<sub>2</sub>P<sub>4</sub>O<sub>12</sub> within the angular overlap model [56–58] led for both compounds to much smaller splittings than those observed.

We understand this mismatch as additional evidence for the strong influence of the vibrational coupling on the electronic absorption spectra of the iron(II) compounds.

In the range of  $16000 \leq \tilde{\nu} \leq 24000$  cm<sup>-1</sup>, rather strong spin-forbidden transitions within the  $[Fe^{II}O_6]$  chromophore are observed. The polarization of these bands is actually responsible for the observed dichroism. A detailed assignment of these spin-forbidden transitions is impossible on the basis of our data. The whole appearance of the observed spectra is, however, very similar to other spectra reported in the literature for the chromophore  $[Fe^{II}O_6]$  (in *e. g.*: MgO:Fe<sup>2+</sup> [59], *vivianite* Fe<sub>3</sub>(PO<sub>4</sub>)<sub>2</sub> · 8 H<sub>2</sub>O [60], *olivine* Fe<sub>2</sub>SiO<sub>4</sub>, *orthopyroxene* and *clinopyroxene* FeSiO<sub>3</sub>, *cordierite* (Mg,Fe)<sub>2</sub>Al<sub>4</sub>Si<sub>5</sub>O<sub>18</sub> · *n* X<sup>Channel</sup>, *alamandine* Ca<sub>3</sub>Fe<sub>2</sub>Si<sub>3</sub>O<sub>12</sub> [61] and references there).

Additionally, bond valence sums were calculated for all atoms of  $\beta$ -FeB<sub>2</sub>O<sub>4</sub>, using the bond length/bond strength concept ( $\Sigma V$ ) [62,63] and the CHARDI concept (*charge distribution in solids*,  $\Sigma Q$ ) [64]. The results of both concepts confirm the supposed formal ionic charges derived from the crystal structure analysis [ $\Sigma V$ : +1.96 (Fe), +2.99 (B), -1.94 (O1), -2.02 (O2), and  $\Sigma Q$ : +2.03 (Fe), +2.98 (B), -1.88 (O1), -2.12 (O2)].

The MAPLE values (*madelung part of lattice energy*) [65–67] were calculated in order to compare them with those of the binary components, *viz.* FeO and the high-pressure modification B<sub>2</sub>O<sub>3</sub>-II. Due to the additive potential of the MAPLE values, it is possible to calculate hypothetical values for  $\beta$ -FeB<sub>2</sub>O<sub>4</sub>, starting from the binary oxides. A value of 26277 kJ mol<sup>-1</sup> was obtained in comparison to 26427 kJ mol<sup>-1</sup> (deviation = 0.57%), starting from the binary oxides (1 × FeO (4489 kJ mol<sup>-1</sup>) [68] + 1 × B<sub>2</sub>O<sub>3</sub>-II (21938 kJ mol<sup>-1</sup>) [69]).

## Conclusions

In this paper, we report the synthesis, crystal structure, and properties of the high-pressure phase  $\beta$ -FeB<sub>2</sub>O<sub>4</sub> in comparison to the data of the isotypic phase HP-NiB<sub>2</sub>O<sub>4</sub>. The structure shows the rare feature of edge-sharing BO<sub>4</sub> tetrahedra, found before in the compounds  $\alpha$ -RE<sub>2</sub>B<sub>4</sub>O<sub>9</sub> (RE = Sm–Ho), RE<sub>4</sub>B<sub>6</sub>O<sub>15</sub> (RE = Dy, Ho), and HP-NiB<sub>2</sub>O<sub>4</sub>. While in the rare-earth compounds only 1/10<sup>th</sup> [ $\alpha$ -RE<sub>2</sub>B<sub>4</sub>O<sub>9</sub> (RE = Sm–Ho)] or 1/3<sup>rd</sup> [RE<sub>4</sub>B<sub>6</sub>O<sub>15</sub> (RE = Dy, Ho)] of the BO<sub>4</sub> tetrahedra are linked *via* a common edge,  $\beta$ -FeB<sub>2</sub>O<sub>4</sub> and its isotype HP-NiB<sub>2</sub>O<sub>4</sub> have BO<sub>4</sub> tetrahedra sharing a common edge with an adjacent BO<sub>4</sub>-unit.

## Acknowledgements

Special thanks go to Prof. Dr. W. Schnick, Department Chemie of the University of Munich (LMU) for the continuous support of this work. We thank T. Miller for collecting the single-crystal data and the temperature-programmed powder diffraction data. We also thank Mr. V. Dittrich, University of Bonn, for his dedicated measurement of the single-crystal absorption spectra. This work was financially supported by the Deutsche Forschungsgemeinschaft (HU 966/ 2-3) and the Fonds der Chemischen Industrie.

- 
- [1] J. S. Knyrim, J. Friedrichs, S. Neumair, F. Roeßner, Y. Floredo, S. Jakob, D. Johrendt, R. Glaum, H. Huppertz, *Solid State Sci.* **2008**, *10*, 168.
- [2] S. C. Neumair, J. S. Knyrim, R. Glaum, H. Huppertz, *Z. Anorg. Allg. Chem.* **2009**, *635*, in press.
- [3] H. Huppertz, G. Heymann, *Solid State Sci.* **2003**, *5*, 281.
- [4] H. Huppertz, *Z. Naturforsch.* **2003**, *58b*, 257.
- [5] H. Emme, M. Weil, H. Huppertz, *Z. Naturforsch.* **2005**, *60b*, 815.
- [6] H. Emme, M. Valldor, R. Pöttgen, H. Huppertz, *Chem. Mater.* **2005**, *17*, 2707.
- [7] J. S. Knyrim, P. Becker, D. Johrendt, H. Huppertz, *Angew. Chem.* **2006**, *118*, 8419; *Angew. Chem. Int. Ed.* **2006**, *45*, 8239.
- [8] H. Huppertz, H. Emme, *Phys.: Condens. Matter* **2004**, *16*, S1283.
- [9] H. Emme, H. Huppertz, *Z. Anorg. Allg. Chem.* **2002**, *628*, 2165.
- [10] H. Emme, H. Huppertz, *Chem. Eur. J.* **2003**, *9*, 3623.
- [11] H. Emme, H. Huppertz, *Acta Crystallogr.* **2005**, *C61*, i29.
- [12] H. Huppertz, B. von der Eitz, *J. Am. Chem. Soc.* **2002**, *124*, 9376.
- [13] H. Huppertz, *Z. Naturforsch.* **2003**, *58b*, 278.
- [14] J. S. Knyrim, F. Roeßner, S. Jakob, D. Johrendt, I. Kinski, R. Glaum, H. Huppertz, *Angew. Chem.* **2007**, *119*, 9256; *Angew. Chem. Int. Ed.* **2007**, *46*, 9097.
- [15] M. Frederico, *Periodico Mineral.* **1957**, *26*, 191.
- [16] J. S. Swinnea, H. Steinfink, *Am. Mineral.* **1983**, *68*, 827.
- [17] N. A. Yamnova, M. A. Simonov, N. V. Belov, *Kristallografiya* **1975**, *20*, 156.
- [18] J. G. White, A. Miller, R. E. Nielsen, *Acta Crystallogr.* **1965**, *19*, 1060.
- [19] R. Diehl, G. Brandt, *Acta Crystallogr.* **1975**, *B31*, 1662.
- [20] J. P. Attfield, A. M. T. Bell, L. M. Rodriguez-Martinez, J. M. Greneche, R. Retoux, M. Leblance, R. J. Cernik, J. F. Clarke, D. A. Perkins, *J. Mater. Chem.* **1999**, *9*, 205.
- [21] J. P. Attfield, A. M. T. Bell, L. M. Rodriguez-Martinez, J. M. Greneche, R. J. Cernik, D. A. Perkins, *Nature* **1998**, *369*, 655.
- [22] J. P. Attfield, J. F. Clarke, D. A. Perkins, *Physica B* **1992**, *180 & 181*, 581.
- [23] T. A. Kravchuk, Y. D. Lazebnik, *Russ. J. Inorg. Chem.* **1967**, *12*, 21.
- [24] I. M. Rumanova, E. A. Genkina, N. V. Belov, *Latv. PSR Zinatnu Akad. Vestis Kimijas Serija* **1981**, *5*, 571.
- [25] R. Diehl, *Solid State Commun.* **1975**, *17*, 743.
- [26] S. C. Neumair, H. Huppertz, *Z. Naturforsch.* **2009**, *64b*, 491.
- [27] T. Kawano, H. Morito, T. Yamada, T. Onuma, S. F. Chichibu, H. Yamane, *J. Solid State Chem.* **2009**, *182*, in press; doi: 10.1016/j.jssc.2009.05.009.
- [28] J. S. Knyrim, H. Huppertz, *J. Solid State Chem.* **2008**, *181*, 2092.
- [29] H. J. Deiseroth, H. Müller-Buschbaum, *Z. Anorg. Allg. Chem.* **1973**, *402*, 201.
- [30] S. Ito, K. Suzuki, M. Iagaki, S. Naka, *Mater. Res. Bull.* **1980**, *15*, 925.
- [31] B. Lazic, V. Kahlenberg, J. Konzett, *Z. Kristallogr.* **2007**, *222*, 690.
- [32] V. Kahlenberg, R. X. Fischer, C. S. J. Shaw, *J. Solid State Chem.* **2000**, *153*, 294.
- [33] N. Kawai, S. Endo, *Rev. Sci. Instrum.* **1970**, *8*, 1178.
- [34] D. Walker, M. A. Carpenter, C. M. Hitch, *Am. Mineral.* **1990**, *75*, 1020.
- [35] D. Walker, *Am. Mineral.* **1991**, *76*, 1092.
- [36] D. C. Rubie, *Phase Transitions* **1999**, *68*, 431.
- [37] H. Huppertz, *Z. Kristallogr.* **2004**, *219*, 330.
- [38] E. Krausz, *Aust. J. Chem.* **1993**, *46*, 1041.

- [39] E. Krausz, *AOS News* **1998**, 12, 21.
- [40] J. W. Visser, *J. Appl. Crystallogr.* **1969**, 2, 89.
- [41] WinXPOW (version 1.2), Stoe & Cie GmbH, Darmstadt (Germany) **2001**.
- [42] X-SHAPE (version 1.05), Stoe & Cie GmbH, Darmstadt (Germany) **1999**.
- [43] W. Herrendorf, H. Bärnighausen, HABITUS, Program for Numerical Absorption Correction, Universities of Karlsruhe and Giessen, Karlsruhe, Giessen (Germany) **1993/1997**.
- [44] G. M. Sheldrick, SHELXS/L-97, program suite for the Solution and Refinement of Crystal Structures, University of Göttingen, Göttingen (Germany) **1997**. See also: G. M. Sheldrick, *Acta Crystallogr.* **2008**, A64, 112.
- [45] The term “sechser” ring was coined by F. Liebau and is derived from the German word “sechs”, which means six. However, a “sechser” ring is not a six-membered ring, but rather a ring with six tetrahedral centers (B) and six electronegative atoms (O). Similar terms exist for rings made up of two or three tetrahedral centers, namely “zweier” and “dreier” rings. See: F. Liebau, *Structural Chemistry of Silicates*, Springer, Berlin, **1985**.
- [46] E. Zobetz, *Z. Kristallogr.* **1990**, 191, 45.
- [47] F. C. Hawthorne, P. C. Burns, J. D. Grice in *Boron: Mineralogy, Petrology and Geochemistry*, (Ed.: E. S. Grew), Mineralogical Society of America, Washington, **1996**.
- [48] M. Ludwig, J. Jäger, R. Niewa, R. Kniep, *Inorg. Chem.* **2000**, 39, 5909.
- [49] G. Cordier, E. Czech, M. Jacowski, H. Schäfer, *Rev. Chim. Mineral.* **1981**, 18, 9.
- [50] S. J. Clarke, F. J. DiSalvo, *Inorg. Chem.* **1997**, 36, 1143.
- [51] M. Somer, W. Carrillo-Cabrera, K. Peters, H. G. von Schnering, *Z. Kristallogr. NCS* **1998**, 213, 230.
- [52] M. Somer, W. Carrillo-Cabrera, K. Peters, H. G. von Schnering, *Z. Kristallogr. NCS* **1998**, 213, 4.
- [53] A. B. P. Lever, *Inorganic Electronic Spectroscopy*, Elsevier Sci. Publ., New York, **1984**.
- [54] R. Glaum, Fe<sub>2</sub>P<sub>4</sub>O<sub>12</sub>, unpublished results, University of Giessen, Giessen **1998**.
- [55] K. Maaß, *Neues von quaternären Phosphaten der zweiwertigen 3d-Übergangsmetalle* (in German), Dissertation, University of Giessen, Giessen **2002**. See: <http://bibd.uni-giessen.de/ghm/2002/uni/d020119.htm>
- [56] C. K. Jørgensen, R. Pappalardo, H. H. Schmidtke, *J. Chem. Phys.* **1963**, 39, 1422.
- [57] D. E. Richardson, *J. Chem. Ed.* **1993**, 70, 372.
- [58] B. N. Figgis, M. A. Hitchman, *Ligand Field Theory and Its Applications*, Wiley-VCH, New York, **2000**.
- [59] K. W. Blazey, *J. Phys. Chem. Solids* **1977**, 38, 481.
- [60] H. U. Güdel, *Inorg. Chem.* **1983**, 22, 3812.
- [61] M. N. Taran, K. Langer, *Phys. Chem. Minerals* **2001**, 28, 199.
- [62] I. D. Brown, D. Altermatt, *Acta Crystallogr.* **1985**, B41, 244.
- [63] N. E. Brese, M. O’Keeffe, *Acta Crystallogr.* **1991**, B47, 192.
- [64] R. Hoppe, S. Voigt, H. Glaum, J. Kissel, H. P. Müller, K. J. Bernet, *J. Less-Common Met.* **1989**, 156, 105.
- [65] R. Hoppe, *Angew. Chem.* **1966**, 78, 52; *Angew. Chem., Int. Ed. Engl.* **1966**, 5, 95.
- [66] R. Hoppe, *Angew. Chem.* **1970**, 82, 7; *Angew. Chem., Int. Ed. Engl.* **1970**, 9, 25.
- [67] R. Hübenthal, M. Serafin, R. Hoppe, MAPLE (version 4.0), Program for the Calculation of Distances, Angles, Effective Coordination Numbers, Coordination Spheres, and Lattice Energies, University of Gießen, Gießen (Germany) **1993**.
- [68] H. Fjellvåg, F. Gronvold, S. Stølen, *J. Solid State Chem.* **1996**, 124, 52.
- [69] C. T. Prewitt, R. D. Shannon, *Acta Crystallogr.* **1968**, B24, 869.
- [70] A. G. Nord, T. Ericsson, P. E. Werner, *Z. Kristallogr.* **1990**, 192, 83.
- [71] A. Olbertz, D. Stachel, I. Svoboda, H. Fueß, *Z. Kristallogr.* **1998**, 213, 241.